JMEPEG (2014) 23:637–642
DOI: 10.1007/s11665-013-0770-1
©ASM International
1059-9495/$19.00

Hardness of FRHC-Cu Determined by Statistical Analysis

J.J. Roa, M. Martínez, E. Rayón, N. Ferrer, F. Espiell, and M. Segarra

(Submitted July 15, 2013; in revised form October 2, 2013; published online November 7, 2013)

A statistical indentation method has been employed to study the hardness value of fire-refined high conductivity copper, using nanoindentation technique. The Joslin and Oliver approach was used with the aim to separate the hardness (*H*) influence of copper matrix, from that of inclusions and grain boundaries. This approach relies on a large array of imprints (around 400 indentations), performed at 150 nm of indentation depth. A statistical study using a cumulative distribution function fit and Gaussian simulated distributions, exhibits that *H* for each phase can be extracted when the indentation depth is much lower than the size of the secondary phases. It is found that the thermal treatment produces a hardness increase, due to the partly re-dissolution of the inclusions (mainly Pb and Sn) in the matrix.

Keywords FRHC copper, cumulative distribution function, nanoindentation

1. Introduction

The worldwide production of copper is around of several thousands of tons per year and its main application is as copper wire, as its most important property is its high electrical conductivity (Ref 1). Copper presents good workability and acceptable values of tensile strength and elongation. The development of a new pirometallurgical process by La Farga Lacambra S.A. (La Farga Group) (Ref 2) leads to a copper with less than 1000 ppm of impurities, obtained from copper scrap, called fire refined high conductivity copper, FRHC-Cu (Ref 3). Its electrical conductivity is higher than 101.2% IACS (International Annealed Copper Standard), which is defined for highly pure copper.

Electrical and mechanical properties can be directly correlated to the composition and microstructure of a material. At nanometric scale, materials present several defects and inclusions, which could modify the mechanical and the electrical (such as the conductivity) properties. Martínez et al. (Ref 4) showed that impurities produce a slightly decrease in copper electrical properties. While, the tensile strength remains quite constant at higher annealing temperatures. Recently, some authors reported several studies on the mechanical properties of copper using different techniques (Ref 5, 6). However, scarce information is available in the literature determining in a statistical way the mechanical response without pile-up effects using nanoindentation technique. In this sense, ultra-low load indentation, is a technique developed over the last decade for probing the mechanical properties of materials (as the hardness and the elastic modulus) at very small scales (Ref 7, 8), but also to locally induce plastic deformation in very small volumes.

Values of the elastic modulus (E) obtained by nanoindentation technique have been reported in the bibliography for different coppers, such as cold-hardened and annealed copper, being the elastic modulus has been found to be 111.8 ± 6.0 and 120.6 ± 4.9 GPa, respectively, at 10 mN of applied load (Ref 9). On the other hand, Shuman et al. (Ref 10) performed cycling load processes on electrolytic copper and studied the evolution of this parameter during the unloading and reloading part of the cycle, yielding values of 166 ± 35.5 and 106 ± 18.7 GPa. Some authors reported that the elastic modulus is strongly modified by the crystallographic orientation (Ref 11). For strain-hardened copper the elastic modulus value varies from 129 to 141 GPa, depending on the crystallographic orientation (Cu (110) and Cu (111), respectively), while for annealed Cu (111) this parameter remains constant and equals to 141 GPa (Ref 12). As can be seen, different elastic modulus are not exactly equal to the value obtained from a tensile test of 110 GPa (Ref 13). This could be related to the pile-up effect induced by the ductile behavior of this metal or maybe due to the anisotropy of this material.

The main purpose of this experimental study is to try to isolate the mechanical properties of the copper matrix and the different superficial defects (inclusions, grain boundaries, etc.) at very small indentation depths (~150 nm) without the need to observe the residual imprints, for FRHC copper with and without thermal treatment, using a statistical method. Thermal treatments modify the mechanical properties of FRHC-Cu at macro scale (Ref 14) and the aim of this work is to determine the true hardness value without any contribution of secondary phases. However, the indentations performed on ductile materials like copper involve plastic deformation, and often the material presents pile-up effects around the residual indentation imprint, yielding an overestimation of the contact area (Ref 15, 16), and producing a strong modification of the mechanical parameters, sometimes by as much as 50% (Ref 17). In the fully plastic regime, the behavior is seen to be dependent on the ratio E/σ_{ys}, where σ_{ys} is the yield

J.J. Roa, Departament de Ciència dels Materials i Enginyeria Metal·lúrgica, CIEFMA-Universitat Politècnica de Catalunya. ETSEIB, Avda. Diagonal, 647, 08028 Barcelona, Spain; **M. Martínez, F. Espiell**, and **M. Segarra**, Departament de Ciència dels Materials i Enginyeria Metal·lúrgica, Centro DIOPMA. Universitat de Barcelona. Facultat de Química, C/ Martí i Franquès, 1, 08028 Barcelona, Spain; **E. Rayón**, Instituto de Tecnología de Materiales, Universidad Politécnica de Valencia, Camí de Vera s/n, 46022 Valencia, Spain; and **N. Ferrer**, La Farga, Ctra. C-17 Km 73.5, Les Masies de Voltregà, 08508 Barcelona, Spain. Contact e-mail: joan.josep.roa@upc.edu.

strength of the material, and the relation between E and σ_{ys} is the strain-hardening of the material. In a low strain-hardening alloy (such as copper), plastically displaced material tends to flow up to and pile-up against to the faces of the indenter, due to the incompressibility of plastic deformation, yielding to an overestimation of the contact area and therefore modifying the mechanical properties (Ref 18). For sharp tip indenters (like Berkovich), indentation with a large amount of pile-up effects can be identified by the distinct blow out at the edges of the contact impression (Ref 19). Due to this effect, accurate measurements of hardnes (H) and elastic modulus (E) cannot be obtained on these materials using the Oliver and Pharr approach (Ref 19-21). In this case, the most useful method to avoid these problems is known as the Joslin and Oliver method (Ref 13). This equation is function of the maximum applied load (P_{max}), the stiffness during the unloading curve (S), the hardness (H), and the effective elastic modulus (E_{eff}), and can be expressed as follows:

$$\frac{4}{\pi}\frac{P_{max}}{S^2} = \frac{H}{E_{eff}^2}. \quad \text{(Eq 1)}$$

The E_{eff} is a parameter which is a function of the elastic properties of the tip indenter and the material of interest. This parameter can be obtained using the equation reported in the literature (Ref 22-24). Equation 1 can be only employed if either the hardness or the elastic modulus is known. Then, the first approach is to try to obtain the elastic modulus for a pure copper sample. For this reason, we have performed an array of 400 indentations at 150 nm of penetration depth for Cu-ETP (Ref 3) (electrolytic tough pitch copper). Afterwards, using the Joslin and Oliver approach (Ref 13), the different hardness values for FRHC copper samples (with and without thermal treatment, which will be indicated by *PH from now on*) had been corrected and recalculated.

2. Experimental Procedure

2.1 Samples Preparation

Samples of different compositions of 8-mm diameter hot-rolled copper wire, from continuous casting supplied by La Farga Lacambra S.A.U. (La Farga Group), were employed. Compositions were determined by an optical emission spectrophotometer (SPECTROLAB-S), and the oxygen content was measured by fusion technique with a LECO oxygen analyzer. Samples correspond to fire-refined high conductivity (FRHC) copper and electrolytic tough pitch copper (ETP). The compositions of the used samples are summarized in Table 1.

One of the FRHC copper samples (PH) has been a thermal treated at its optimal pre-heating temperature for one hour as described elsewhere (Ref 12). Copper specimens were polished with silicon carbide and diamond suspension of 30, 6, and 3 μm. Finally, a neutral suspension of 20-nm alumina particles was used in order to remove possible work hardening introduced during surface preparation.

2.2 Mechanical Properties

Nanoindentation tests were performed with a Nano Indenter® XP System (Agilent Technologies) with a constant strain rate held at 0.05 s^{-1}. The experiments were performed on the transversal section of the different samples using a diamond Berkovich tip. The indenter shape has been carefully calibrated for true indentation depths as small as 50 nm by indenting fused silica samples with a well known elastic modulus of 72 GPa (Ref 14). The nanoindenter experiments were performed at a constant indentation depth in order to isolate the contribution of each phase of interest (copper and the rest, considered as a unique phase, which includes inclusions and grain boundaries (GB)) to the mechanical properties of the whole sample. To insure there was a sufficient population of tests to conduct a statistical study, an array of 20×20 indentations with 1 μm spacing was performed at 150 nm of indentation depth. The unloading segment of the *P-h* curve was employed for the extraction of mechanical properties, based on the Oliver and Pharr method (Ref 14, 17, 18).

3. Statistical Method

Here the important parameter to take into account is the indentation depth, h. When tests are performed at high indentation depths, the imprint tends to be higher than the size of the secondary phases, and the obtained response corresponds to that of the whole material with the contribution of all phases present in the material of study. On the contrary, for low indentation depths, the contribution of each of the phases present in the sample can be isolated, and thus their mechanical properties can be separately obtained due to the small size of the residual imprint, which is lower than the secondary phase size (Ref 25-28). Furthermore, it is important to mention that a large number of imprints will increase the accuracy of the results, as expected for any experiment.

If we consider a sample composed by several j distinct phases with different mechanical properties, and we assume that the distribution (p_j) of the mechanical property (x), e.g. H, of each of these j phases is considered to obey a Gaussian distribution (Ref 25-27, 29), which follows the next equation:

$$p_j = \frac{1}{\sqrt{2\pi\sigma_j^2}}\exp\left(-\frac{(x-\mu_j)^2}{2\sigma_j^2}\right) \quad \text{(Eq 2)}$$

where σ_j is the standard deviation and μ_j the arithmetic mean or average for all of the number of indentations (N_j), performed on each material phase (j). The cumulative distribution function can be written as:

$$\text{CDF} = \sum_j \frac{1}{2} f_j \text{erf}\left(\frac{x-x_j}{\sqrt{2}\sigma_j}\right) \quad \text{(Eq 3)}$$

where x is the mechanical property (H in our case), x_j is the hardness for each phase j, and f_j is defined as the relative fraction occupied by each phase and defined as follows:

Table 1 Chemical composition of the investigated copper (wt.%)

Sample	Sn	Zn	Pb	Ni	Fe	Sb	Ag	ΣIt	O_2
ETP	0.7	1.5	1.1	1.5	17.1	1.0	11.1	38.0	170.0
FRHC	151.0	46.0	425.0	53.0	7.0	26.0	45.0	749.0	228.0

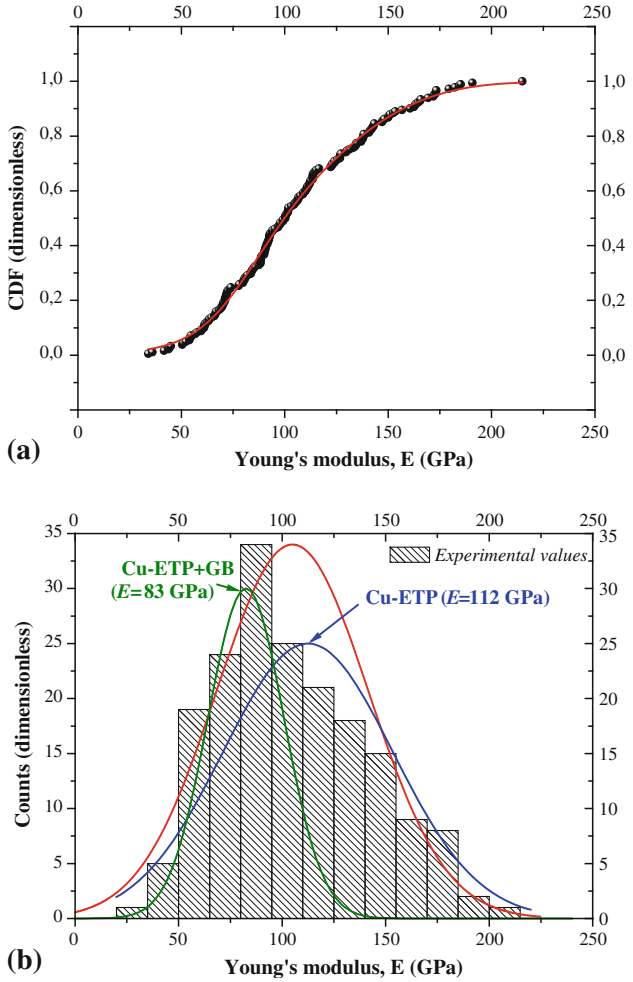

Fig. 1 (a) Statistical analysis to determine the elastic modulus for a pure copper sample (Cu-ETP), and (b) elastic modulus determined from 400 indents performed with a 150 nm of indentation depth at the same sample

$$f_j = \frac{N_j}{N} \quad \text{(Eq 4)}$$

where N_j corresponds to the number of indentations performed on each phase, and N is the total number of imprints performed on the sample of study. This relative fraction must also obey the following equation (Ref 30):

$$\sum_{j=1}^{n} f_j = 1 \quad \text{(Eq 5)}$$

4. Results and Discussion

In order to observe, discuss, and clarify these results without the influence of the bin size, the different results were represented by cumulative density functions, by assuming that the density functions are correctly fitted by Gaussian distributions. This approach has also been reported in previous studies performed on heterogeneous materials (Ref 23-26). The mean value for hardness, μ_j^H, and the standard deviation, σ_j^H, were obtained by fitting the cumulative distribution functions (CDF), using a special sigmoid shape error function, defined in Eqs 2 and 3. Figure 1(a) shows the plot of the CDF versus elastic modulus. For our materials with two different phases (copper matrix and inclusions plus GB) Eq 3 for hardness can be rewritten as follows:

$$f(H) = CDF = \frac{1}{2} f_{\mathrm{Cu}} \mathrm{erf}\left(\frac{H - H_{\mathrm{Cu}}}{\sqrt{2}\sigma_{\mathrm{Cu}}^H}\right) + \frac{1}{2} f_{\mathrm{inclusions+GB}} \mathrm{erf}\left(\frac{H - H_{\mathrm{inclusions+GB}}}{\sqrt{2}\sigma_{\mathrm{inclusions+GB}}^H}\right). \quad \text{(Eq 6)}$$

Table 2 Summary of the CDF fitting

	Samples		
Parameters	**Cu-ETP**	**Cu-FRHC with PH**	**Cu-FRHC without PH**
E_s (GPa)	112.460 ± 3.002	-	-
f_s (%)	72.857 ± 5.172	-	-
σ_s (GPa)	40.979 ± 1.239	-	-
E_{GB} (GPa)	82.532 ± 1.230	-	-
f_{GB} (%)	27.143 ± 5.610	-	-
σ_{GB} (GPa)	18.393 ± 2.130	-	-
H_s (GPa)	-	1.936 ± 0.001	1.369 ± 0.002
f_s (%)	-	81.068 ± 2.878	94.295 ± 1.980
σ_s (GPa)	-	0.114 ± 0.0426	0.0935 ± 0.003
H_{i+GB} (GPa)	-	1.634 ± 0.109	1.0750 ± 0.053
f_{i+GB} (%)	-	18.932 ± 4.260	5.701 ± 1.980
σ_{i+GB} (GPa)	-	0.4119 ± 0.048	0.114 ± 0.041
χ^2	$1.869.10^{-4}$	$3.19.10^{-4}$	$4.28.10^{-4}$
R^2	0.9977	0.9990	0.9987

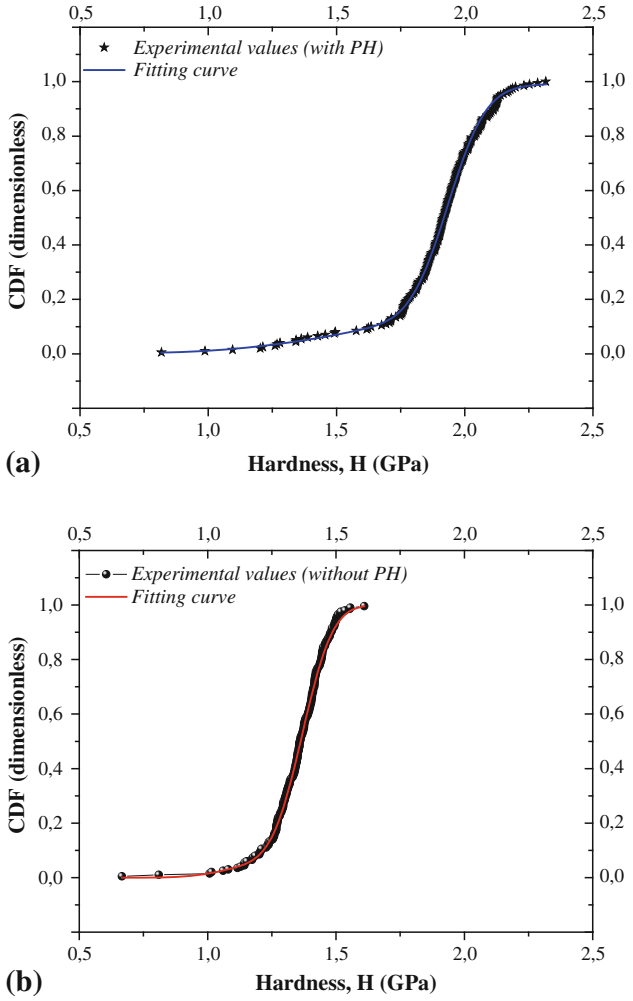

Fig. 2 Statistical analysis to determine the Hardness value for a copper with impurities (a) samples with thermal treatment (PH), and (b) samples without PH

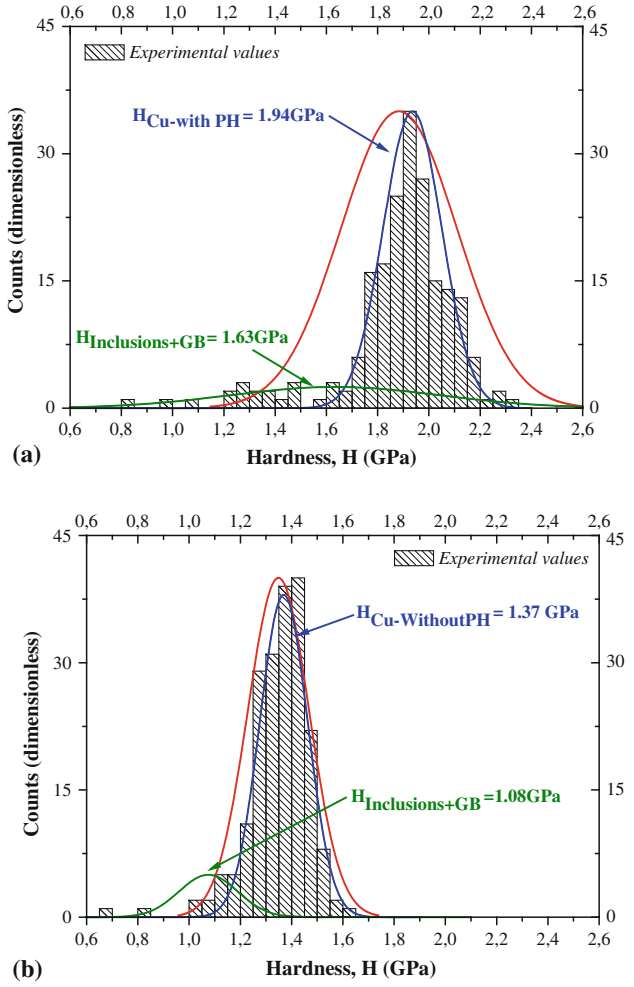

Fig. 3 Hardness determined from 200 indents performed with a 150 nm of indentation depth (a) samples with PH, and (b) samples without PH

During the deconvolution process, in which Eq 6 was used to obtain the hardness of each phase, several restrictions were programmed in order to obtain an accurate value: the sum of the total area (f_j) or the surface fraction of each phase was set at 1 (Eq 5), and the fitting process was programmed to be completed when the tolerance of the chi-square (χ^2) was less than 1×10^{-15}. The different results after the fitting process for the Cu-ETP sample can be observed in Table 2. As can be seen, the obtained value for the elastic modulus for the copper matrix is around 110 GPa, which is in agreement with the reference (Ref 11).

After that, we plot the experimental values in the form of a histogram and simulate the different values obtained after the fitting process, see Fig. 1(b). In this case, only two different phases have been taken into account: one corresponding to the copper matrix contribution (the majority phase with a relative frequency of 73% and elastic modulus of 112 GPa) and the other related to the interaction between the copper matrix and the other phases including inclusions and grain boundaries, GB, (with a relative frequency of 27% and elastic modulus of 83 GPa). We can observe that the interaction of the matrix with the rest of the phases produces a reduction around 36% of the elastic modulus.

Figures 2(a) and (b), exhibit the *CDF* versus the hardness and the correspondent fittings of these values for FRHC copper samples with and without thermal treatment. The results are summarized in Table 2. The histograms of hardness values for both samples, measured at the same indentation depth, are plotted in Fig. 3(a) and (b), with a 0.5 GPa bin size. As for the elastic modulus of the Cu-ETP, two main peaks are observed for each FRHC sample, the highest ones centered at 1.94 and 1.37 GPa, for FRHC copper with and without thermal treatment, respectively. This can be related to the pure copper phase. Furthermore, in both, histograms secondary hardness peaks appear at 1.63 and 1.08 GPa for the same samples, respectively. Their position in the histogram is not the same for each sample, thus indicating that inclusions, grain boundaries and/or other phases are present in a different percentage or size, see Fig. 4.

The thermal treatment can produce a considerable increase in grain size, the formation of different phases and mainly the change in the crystal structure and other mechanisms which help to increase the hardness of the material. An EDX analysis shows that the different inclusions present in Fig. 4(a, b) contain Pb and/or Sn. As can be observed in Fig. 3, the sample with thermal treatment is harder than the other. This increment could be related to the re-dissolution process of the Pb and Sn inclusions inside of the matrix (solid solution), thus producing an increasing of the hardness value. Furthermore, due to the small percentages of elements in the copper matrix, the microstructure of a material may change due to dislocations movement. However, one of the

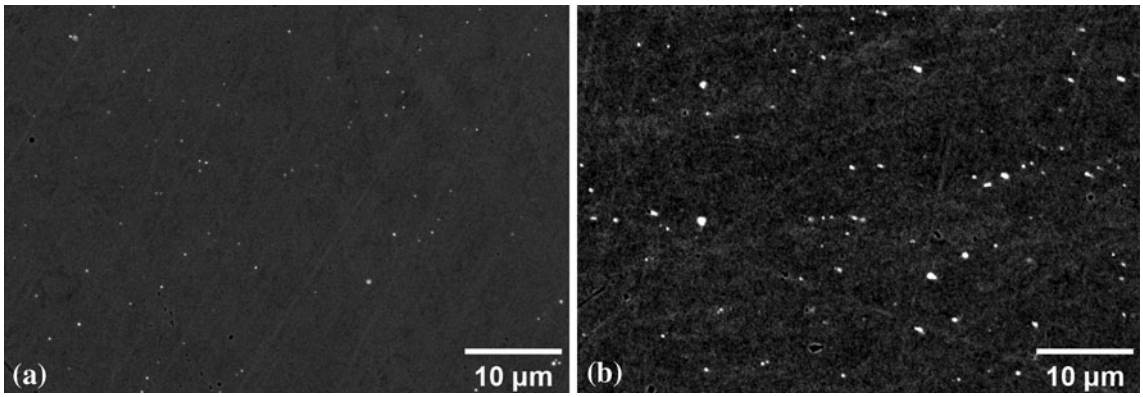

Fig. 4 SEM image ×1000 of the different samples of study, showing the high amount of inclusions (a) samples without PH, and (b) samples with PH

main factors, which can produce a strong modification of the hardness value, is that the dislocation activity (formation and sliding) no longer dominates the plastic deformation, being grain-boundary sliding and/or grain rotation anticipated, thus varying the mechanical properties.

The different hardness values reported in Table 2 are in correct agreement with the results published by Zhang et al. (Ref 31), which yield a range between 1150 MPa (for coarse-grained copper) to 1450 MPa (for dynamic plastic deformation of copper at liquid nitrogen temperature).

5. Conclusions

The statistical method of H and E cumulative distribution functions enables the depiction of the mechanical response for each constituent phase, as a normal density function.

In summary, nanoindentation has been used to characterize the mechanical properties of different copper samples with different microstructures. The statistical method allows isolating the mechanical properties of the different phases present in each sample. Moreover, this method is very efficient to detect the presence of grain boundaries or inclusions when the test is performed at indentation depths producing imprints with sizes smaller than the size of the other phases different from copper matrix.

The thermal treatment produces a hardness increase, due to the partly re-dissolution of the inclusions (Pb and Sn) in the matrix. Moreover, these inclusions may produce a change in the microstructure thus generating a partial movement of dislocations inside of the copper matrix.

Acknowledgments

The corresponding authors would like to thank La Farga Lacambra Group for the materials supplied. Furthermore, the authors would like to thank the Linguistic Services at the University of Barcelona for linguistic and stylistic advice.

References

1. A. Esparducer, M.A. Fernandez, M. Segarra, J.M. Chimenos, and F. Espiell, Characterization of Fire-Refined Copper Recycled from Scrap, *J. Mater. Sci.*, 1999, **34**, p 4239–4244
2. http://www.lfl.es/esp/default.asp. Accessed on 27 Dec 2012
3. http://www.copper.org/. Accessed on 27 Dec 2012
4. M. Martínez, A.I. Fernández, M. Segarra, H. Xuriguera, F. Espiell, and N. Ferrer, Comparative Study of Electrical and Mechanical Properties of Fire-Refined and Electrolytically Refined Cold-Drawn Copper Wires, *J. Mater. Sci.*, 2007, **42**, p 7745–7749
5. L.E. Murr, Correlating Impact Related Residual Microstructures Through 2D Computer Simulations and Microindentation Hardness Mapping: Review, *Mat. Sci. Technol.*, 2012, **28**, p 1108–1126
6. Armstrong, R.W., Elban, W.L., and Walley, S.M. Elastic, Plastic, Cracking Aspects of the Hardness of Materials. Int. J. Mod. Phys. B., 2013, **27**(8), p 1330004 (79 pp). doi:10.1142/S0217979213300041
7. M.F. Doerner and W.D. Nix, A Method for Interpreting the Data from Depth-Sensing Indentation Instruments, *J. Mater. Res.*, 1986, **1**, p 601–609
8. G.M. Pharr and W.C. Oliver, Measurement of Thin Film Mechanical Properties Using Nanoindentation, *MRS Bull.*, 1992, **17**, p 28–33
9. M.F. Doerner, D.S. Gardner, and W.D. Nix, Plastic Properties of Thin Films on Substrates as Measured by Submicron Indentation Hardness and Substrate Curvatures Techniques, *J. Mater. Res.*, 1986, **1**, p 845–851
10. D. Shuman, A. Costa, and M. Andrade, Calculating the Elastic Modulus from Nanoindentation and Microindentation Reload Curves, *Mater. Charact.*, 2007, **58**(4), p 380–389
11. M. Magnuson, M. Mattesini, C. Li, C. Höglund, M. Beckers, L. Hultman, and O. Eriksson, Bonding Mechanism in the Nitrides Ti_2AlN and TiN: An Experimental and Theoretical Investigation, *Phys. Rev. B*, 2007, **76**, p 195127/1–195127/9
12. K.W. McElhaney, J.J. Vlassak, and W.D. Nix, Determination of Indenter Tip Geometry and Indentation Contact Area for Depth-Sending Indentation Experiments, *J. Mater. Res.*, 1998, **13**, p 1300–1306
13. W.D. Callister, Jr., *Introduccion a la Ciencia e Ingenieria de los Materiales*, Ed. Reverté S.A, Barcelona, 2005
14. A. Esparducer, M. Segarra, F. Espiell, M. Garcia, and O. Guixà, Effects of Pre-heating Treatment on the Annealing Behaviour of Cold-Drawn Fire-Refined Coppers, *J. Mater. Sci.*, 2001, **36**, p 241–245
15. D.L. Joslin and W.C. Oliver, A New Method for Analyzing Data from Continuous Depth-Sensing Microindentation Tests, *J. Mater. Res.*, 1990, **5**, p 123–126
16. W.C. Oliver and G.M. Pharr, An Improved Technique for Determining Hardness and Elastic Modulus Using Load and Displacement Sensing Indentation Experiments, *J. Mater. Res.*, 1992, **7**, p 1564–1583
17. A. Esparducer, M. Segarra, F. Espiell, M. Garcia, and O. Guixà, Effects of Pre-heating Treatment on the Annealing Behaviour of Cold-Drawn Fire-Refined Coppers, *J. Mater. Sci.*, 2001, **36**, p 241–245
18. J.S. Field and M.V. Swain, A Simple Predictive Model for Spherical Indentation, *J. Mater. Res.*, 1993, **8**, p 297–306
19. W.C. Oliver and G.M. Pharr, Review: Measurement of Hardness and Elastic Modulus by Instrumented Indentation: Advances in Understanding and Refinements to Methodology, *J. Mater. Res.*, 2004, **19**, p 3–20
20. G.M. Pharr, Measurement of Mechanical Properties by Ultra-Low Load Indentation, *Mater. Sci. & Eng. A.*, 1998, **253**, p 151–159
21. J.L. Hay and G.M. Pharr, Instrumented Indentation Testing, *ASM Handbook*, 2000, **8**, p 232–243

22. S. Suresh, T.G. Nieh, and B.W. Choi, Nano-indentation of Copper Thin Films on Silicon Substrates, *Scr. Mater.*, 1999, **41**, p 951–957
23. A. Gouldstone, H.J. Koh, K.Y. Zeng, A.E. Giannakopoulos, and S. Suresh, Discrete and Continuous Deformation During Nanoindentation of Thin Films, *Acta Mater.*, 2000, **48**, p 2277–2295
24. J. Chen, W. Wang, L.H. Qian, and K. Lu, Critical shear stress for onset of plasticity in a nanocrystalline Cu determined by using nanoindentation. Scr. Mater., 2003, **49**, pp. 645-650; **48**, pp. 2277-2295
25. G. Constantinides, F.J. Ulm, and K. Van Vliet, On the use of nanoindentation for cementitious materials, *Mater. Struct.*, 2003, **36**, p 191–196
26. G. Constantinides and F.J. Ulm, The nanogranular nature of C-S-H, *J. Mech. Phys. Sol.*, 2006, **55**, p 679–690
27. G. Constantinides, K.S. Ravi Chandran, F.J. Ulm, and K. Van Vliet, Grid Indentation Analysis of Composite Microstructure and Mechanics: Principles and Validation, *Mater. Sci. Eng., A*, 2006, **430**, p 189–202
28. N.X. Randall, M. Vandamme, and F.-J. Ulm, Nanoindentation Analysis as a Two-Dimensional Tool for Mapping The Mechanical Properties of Complex Surfaces, *J. Mater. Res.*, 2009, **24**(3), p 679–690
29. V. Canseco, J.J. Roa, E. Rayón, A.I. Fernandez, and E. Palomo, Mechanical Characterization at Nanometric Scale for Heterogeneous Graphite-Salt Phase Change Materials with a Statistical Approach, *Ceram. Inter.*, 2012, **38**(1), p 401–409
30. F.J. Ulm, M. Vandamme, C. Bobko, J. Alberto Ortega, K. Tai, and C. Ortiz, Statistical Indentation Techniques for Hydrated Nanocomposites: Concrete, Bone, and Shale, *J. Am. Ceram. Soc.*, 2007, **90**, p 2677–2692
31. Y. Zhang, N.R. Tao, and K. Lu, Mechanical Properties and Rolling Behaviours of Nano-Grained Copper with Embedded Nano-twin Bundles, *Acta Mater.*, 2008, **56**, p 2429–2440